SWIFT-UVOT-CALDB-17-01b
Date Original Submitted: 2015-10-15
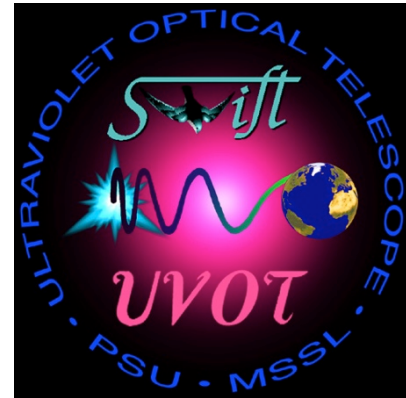Prepared by: A. A. Breeveld
Date Revised: 2016-10-10
Revision #1
Revised by: A.A.Breeveld
Sections Changed: added 3.3
Comments: Added a link to where the tools and
instructions can be found.

SWIFT UVOT CALDB RELEASE NOTE

SWIFT-UVOT-CALDB-17: Small Scale Sensitivity

0. Summary:

This CALDB product should give a correction for small regions of low sensitivity for
each filter. At present there is no well-defined correction so instead any sources
falling on these regions are recognised by an SSS factor value of -99.9.

1.   Component Files:

FILE NAME	VALID DATE	RELEASE DATE	VERSION

2. Scope of Document:

This document includes a description of the product, expected future updates,
warnings for the user, a list of data the product is based on and finally the analysis
methods used to create the product.

Other relevant documents are "SWIFT-UVOT-CALDB-15: Sensitivity loss"
(uvotcaldb_throughput_03.pdf) and "UVOT Small Scale Sensitivity Regions"
(sss_patches_v4.pdf).

3. Changes:

This is the first release of a calibration for this product. Small areas of low sensitivity
have recently been defined for the UVOT for the first time.

3.1.   CALDB file versions:

Version 1 (sssfile4.fits)

3.2. CALDB content:

In this version the areas of low sensitivity are given the factor -99.9. When the SSS file is used, the final magnitudes for any sources falling in these areas are given the value NULL and corrected count rates appear negative.

3.3. Using CALDB

The CALDB file and directions for using it can be found on the UVOT digest page at:
http://swift.gsfc.nasa.gov/analysis/uvot_digest/sss_check.html

4. Reason For Update:
Sources falling within the small-scale areas of low sensitivity can give count rates of up to 34% lower than in other areas.

5. Expected Updates:

We expect to replace the -99.9 factor with real correction factors so that sources falling in the affected areas do not have to be discarded.

6. Caveat Emptor:

Some of the regions are defined crudely as rectangles so some source count rates might be discarded that are actually ok. Similarly low count rates may be found in other areas that are not yet known to have low sensitivity.

7. Data Used:

- White dwarfs used for throughput trending (listed in Table 1)
- Many repeated observations of the AGN NGC5548 (Table 1)
- Scattered light images (i.e. summed images of the sky background with sources removed)
- LED flat fields.

source	RA	Dec
WD1026+453	10 29 45.3	+45 07 03.0
WD1121+145	11 24 15.9	+14 13 49.0
WD1657+343	16 58 51.3	+34 18 51.0
NGC5548	14 17 59.51	+25 08 12.5

Table 1 Specific sources used for SSS

8. Description of Analysis:

NGC 5548

Recent intensive sampling (~ 4 months of approximately 2 per day) of the AGN NGC5548 showed some anomalous abrupt, short-lived dips in count rate that are physically implausible. These dips are seen mainly in the UV filters, with the deepest

in UVW2 (by up to 34% in W2, 22% in M2, 17% in W1) (see Figure 1). The dips are weaker in the optical bands. Other stars in the field do not show corresponding dips in their light curves and HST UV data on the same object does not have similar dropouts. Although NGC5548 is a variable source the sheer volume of data has allowed the problem to be pinpointed.
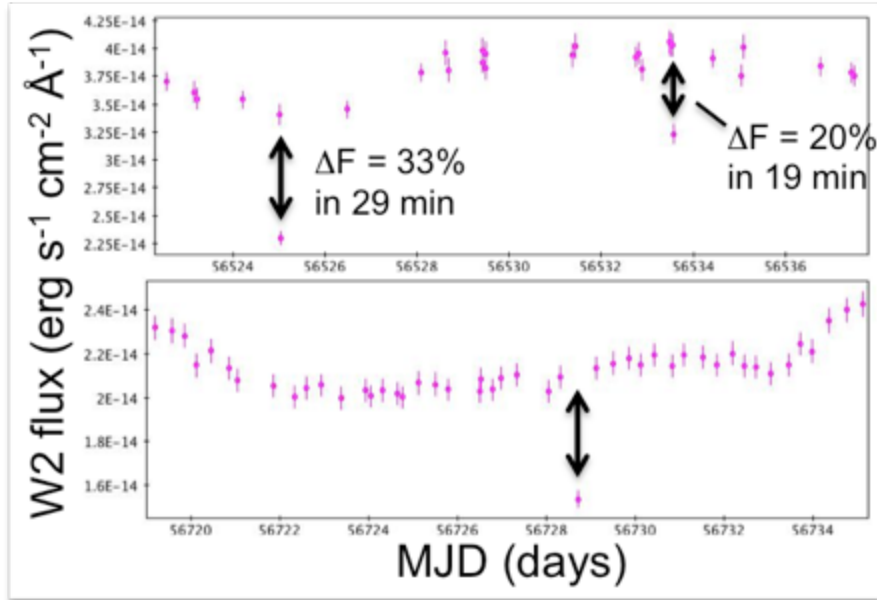

Figure 1 From Gelbord et al. (2014)*: UVW2 light curves of NGC 5548 showing dips. Top: two very rapid dips that are difficult to explain physically. Bottom: dip timescale contrasts sharply with other variability in this band.

The data were checked for any known problems (no image artifacts, elevated backgrounds, tracking errors, etc.).

Gelbord et al. (2014)* identified 85 dips by comparing fluxes to neighbouring values in the light curves and found them to be clustered in raw detector coordinates. The raw coordinates were calculated from the sky coordinates using the telescope pointing parameters. This transformation did not include the distortion map, but even without this correction it was clear that the points lie in certain positions (see Figure 2). Thus there appear to be localised regions of reduced sensitivity.

Edelson and Gelbord (private communication) defined boxes containing most of the major clusters of bad points (see Table 2). The boxes cover ~4% of the central 5' x 5' of the UVOT field (0.4% of whole field of view), implying that a few percent of UVOT measurements may be affected.

---

* Gelbord et al. 2014, Proceedings of Swift: 10 Years of Discovery (SWIFT 10), held 2-5 December 2014 at La Sapienza University, Rome, Italy. Online at
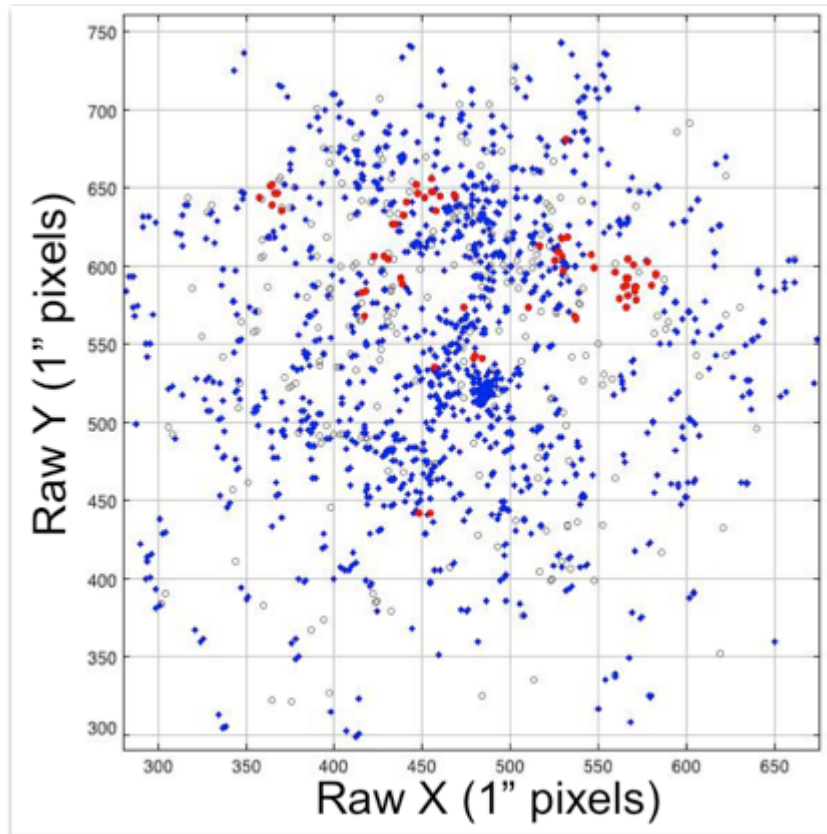http://pos.sissa.it/archive/conferences/233/137/SWIFT%2010_137.pdf

Figure 2 : From Gelbord et al. (2014): Measurements in the detector plane, showing the clustering of verified dips (red circles). Non-dipping flux values are blue diamonds; measurements lacking neighbours within ±2 days are untested (grey open circles).

Xcent	Ycent	Dx	Dy
728	1285	28	34
855	1214	50	100
910	1289	56	42
905	882	18	4
963	1081	10	6
1053	1215	42	46
1074	1132	4	8
1128	1180	76	68

Table 2 Showing the location in full resolution raw subpixels of the most recently defined 8 boxes. They are shown in Figure 4.

White Dwarf measurements

The throughput trending in the UV uses three White Dwarf standards. These have occasionally given unbelievably low values, and these outlying values have been removed manually from the data set. Since the early days the trending observations have been measured using sky images however, now using the python routine convertsky2det2raw it is possible to see that in nearly all cases the anomalous points in raw coordinates lie on the regions of low sensitivity. Comparing the raw coordinates with the box positions has now helped eliminate more suspect

measurements from the trending. However, conversely there are still some low WD measurements that do not lie in the boxes.

LED flat fields

In order that the detector may be calibrated in flight, four flood-LEDs are provided. They are located off-axis close to the detector and are positioned so that their emission falls on the side of the filter facing the detector. The blank filter is put in place, which then acts as a defocused "screen" providing the flat field. They are green LEDs but with emission in the UV range (Huckle, 2006). The illumination is fairly even and these images are known as LED flat fields although the illumination is not totally flat. The images are smoothed over the large-scale and summed to make deep images of more than 10^{10} counts. These images do show some stable variation in brightness on a subpixel scale and are used annually to identify bad pixels and by comparing new images with previous ones, any areas where the throughput has declined with time and usage are identified. However, these areas do not correspond with those found by NGC5548 and nothing new showed up in the 2014 LED flat field data.

The regions of low sensitivity described above do not coincide with already-identified bad pixels. Bad pixels are identified from the LED flat fields as having a count rate in a CCD pixel more than 3 sigma from the mean (see badpixel document: SWIFT-UVOT-CALDB-01). Looking at a higher resolution scale of subpixels and relaxing the criteria to include bad subpixels with less than 3 sigma from the mean still did not produce any better correlation with these regions.

Directly comparing the LED flat field count rates inside the regions with those outside did not show anything useful. Thus it appears that the LED flats do not show the same regions of reduced sensitivity. The regions only show up in images taken of the sky.

Scattered light background images

For the Breeveld et al. 2010 paper we created images of the diffuse scattered light by taking many full frame images from the archive and masking out all sources, ghost images and readout streaks to leave just the background light. Unbinned raw images for each filter were summed together using the background level and mask maps to normalise the values in each pixel. The resulting images (shown in Fig 20 of Breeveld et al. 2010) reveal the scattered light rings and central enhancement. In addition several small dark patches are seen at identical positions for each filter, but with slightly different patterns for the Optical and UV filters. The number of counts per pixel in these patches is up to a few percent lower (10% at most) than in the surrounding regions.

The clusters of bad points located in the NGC5548 data coincide with these patches (see Figure 3).
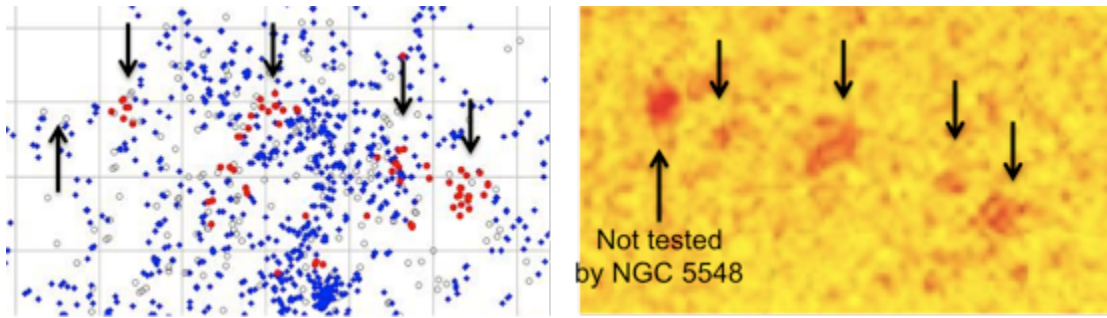
Figure 3 From Gelbord et al. 2014: A comparison of the distribution of flux outliers to blemishes in a source-subtracted UVM2 background image (Breeveld et al. 2010, MNRAS 406, 1687).

The matching up of the boxes with the patches shows up best with UVM2 (see Figure 4). In the other cases the scattered light ring apparently 'masks' the patches (or maybe simply swamps them). In the optical filters there are hints of patches at the same positions, but there are other deeper patches in different positions (see Figure 5). The dropouts in the optical seem to be less of a problem and less deep.
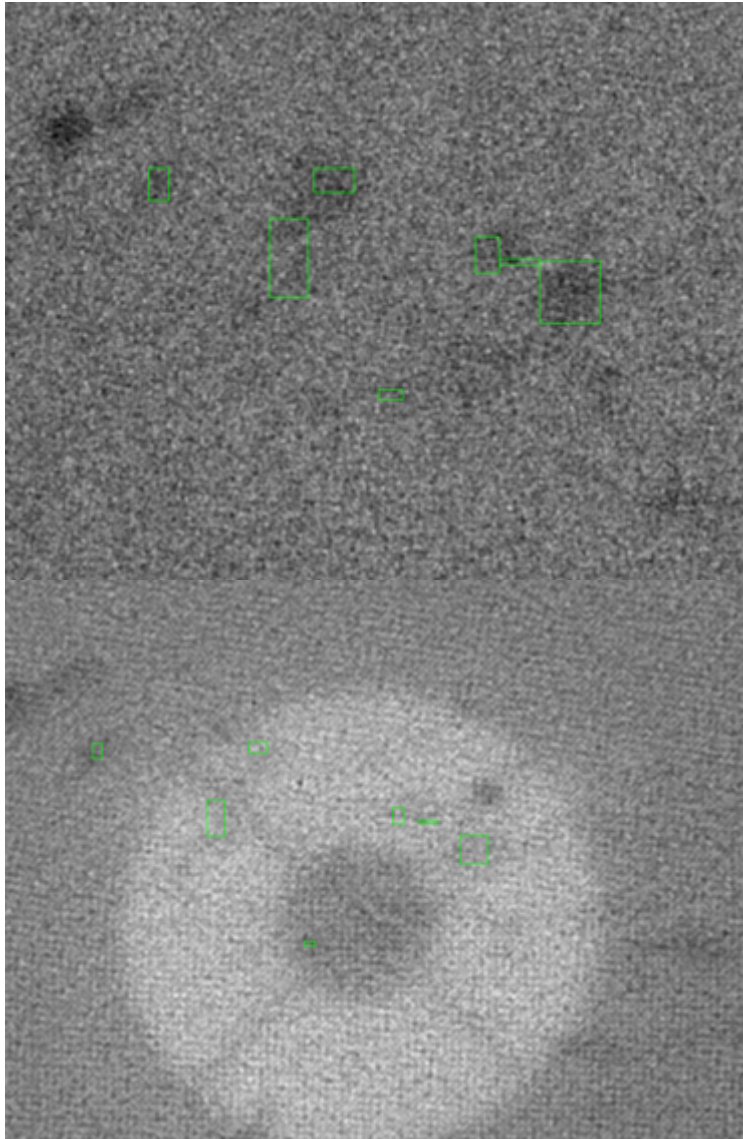
Figure 4 The central regions of two scattered light images. Top, UVM2 and bottom, UVW1. The same patches are visible in both, but in UVW1 some of them are partially obscured by the scattered light ring. The first set of 7 boxes (defining the low NGC5548 points) are overplotted on each.
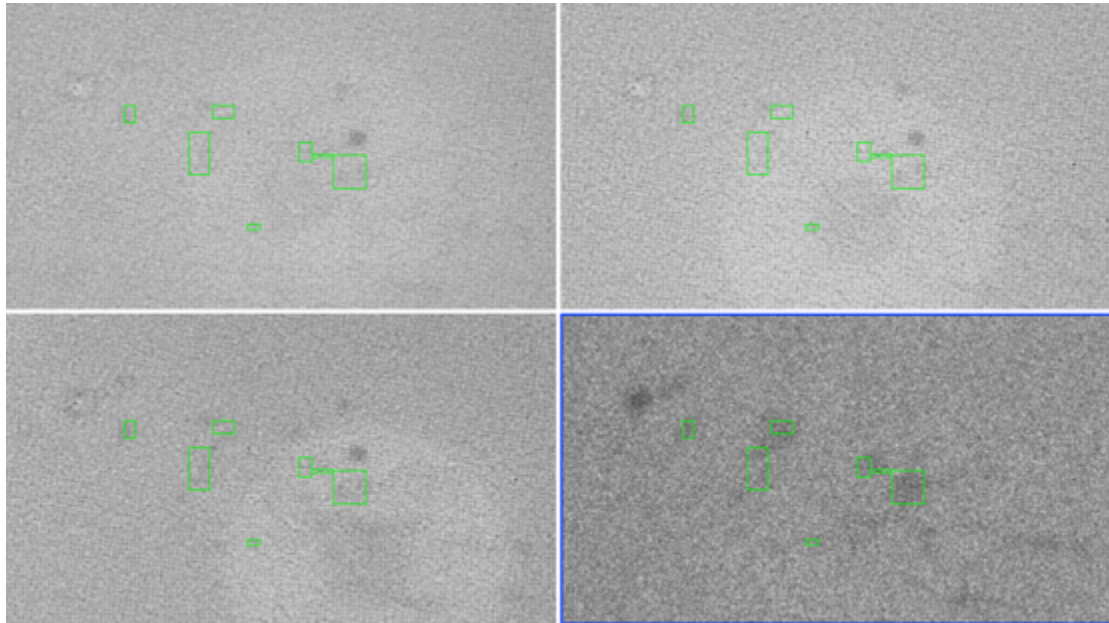
Figure 5 Showing the difference between the patches in optical filters with those UVM2. From top left, V,B,U,UVM2.

Although some of the patches appear to be swamped in the UVW1 and UVW2 filters by scattered light, dropouts are still measured in these regions. Figure 6 shows the NGC5548 measurements from all the UV filters overlaid on the UVM2 scattered light image. Similarly there is a dark patch low down in the optical images that doesn't seem significant in the UV, but the yellow points marked with an arrow in Figure 6 line up with that patch.
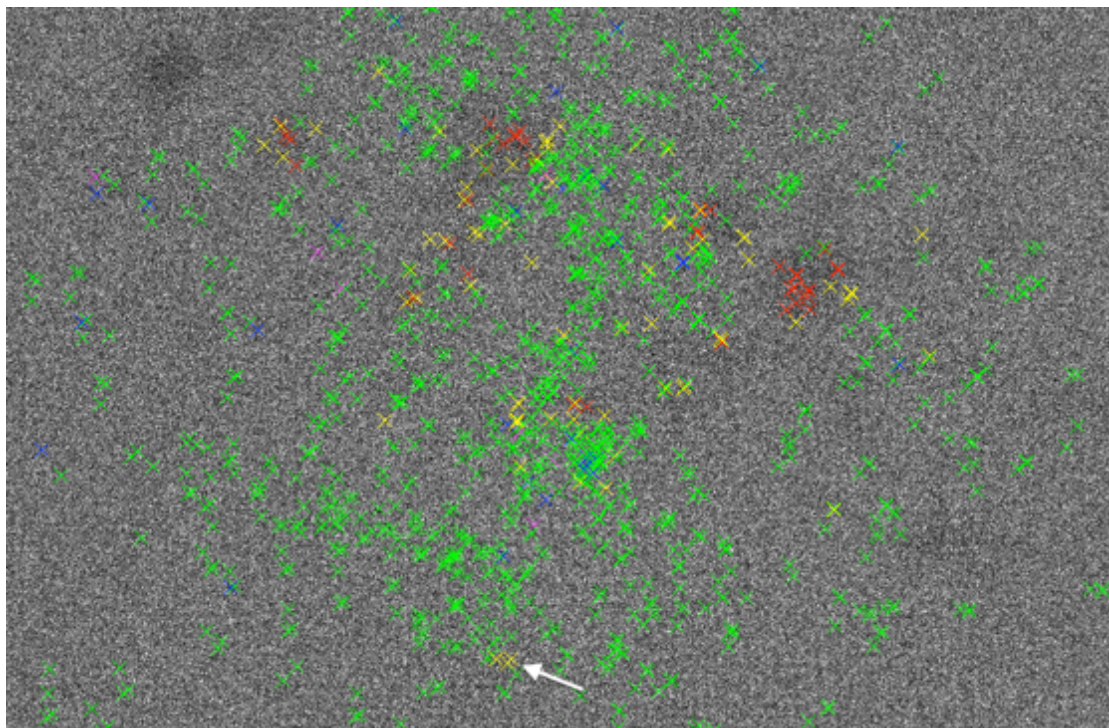

Figure 6 UVM2 scattered light image overlaid with NGC5548 measurements. The red crosses are the deepest dropouts with more than 10% reduction, yellow are around 5% reduction, green ok. Blue and purple mark rates that are high compared with the mean. The arrow points to the position of a patch in the optical images that is barely seen in the UV.

8.1. Dust on photocathode

It is believed that the regions of low sensitivity are caused by dust or other debris lying loosely on the surface of the photocathode. The collimated light coming from the telescope is scattered by the debris, leaving a shadow, whereas diffuse light from the LED is coming from sufficiently random directions not to create the shadow. This also explains why the scattered light seems to be differently affected; the scattered light reaches the detector via a different pathway. The debris material is apparently of a size or nature to absorb the UV light more than optical.

It has to be noted that cleanliness during the manufacture and build of the detector and telescope was taken with the utmost importance and seriousness, hence the improved throughput in the UV for the UVOT compared with the XMM-OM in which some contamination occurred. Nevertheless some contamination cannot be ruled out.

9. Correcting the measured count rates

Since the optical and UV patches have slightly different patterns, there are two sets of SSS maps: one for the optical (plus *white*) and one for the UV. These were made initially by smoothing and filtering the best scattered light images to get the dark patches. Some dropout positions were outside these patches, so the rectangles defined from NGC5548 were added as well for safety. Figures 7 and 8 shows the bad patches defined in this product. The SSS factor is unity over the whole field except for the black patches which have a factor of -99.9.
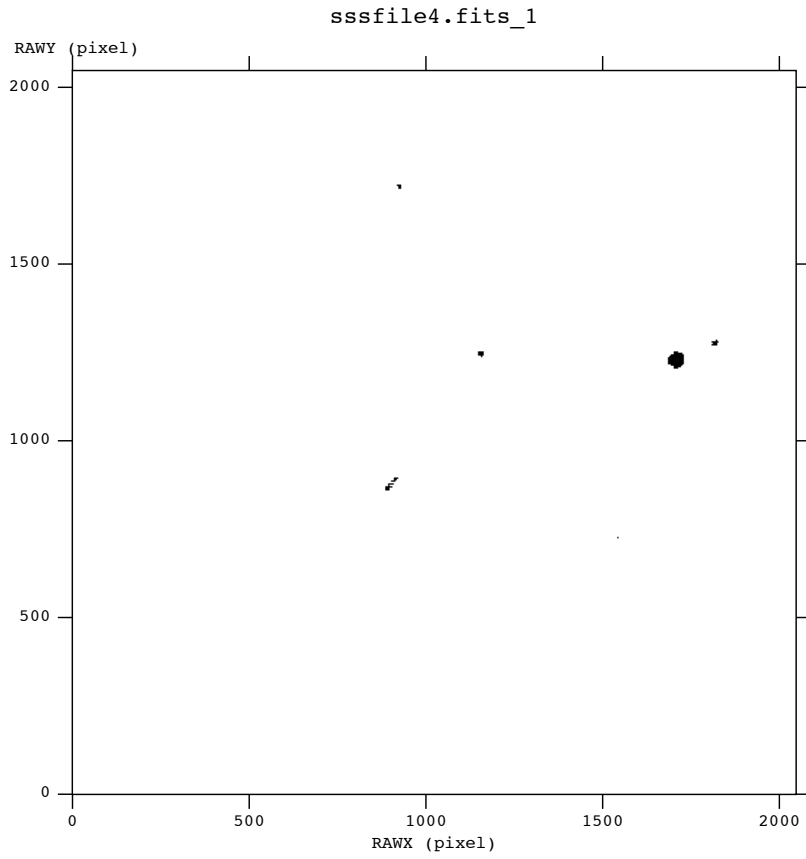The SSS maps for the grisms have been left at unity for now.

Figure 7 SSS map for optical and white filters. Regions of low sensitivity are in black.
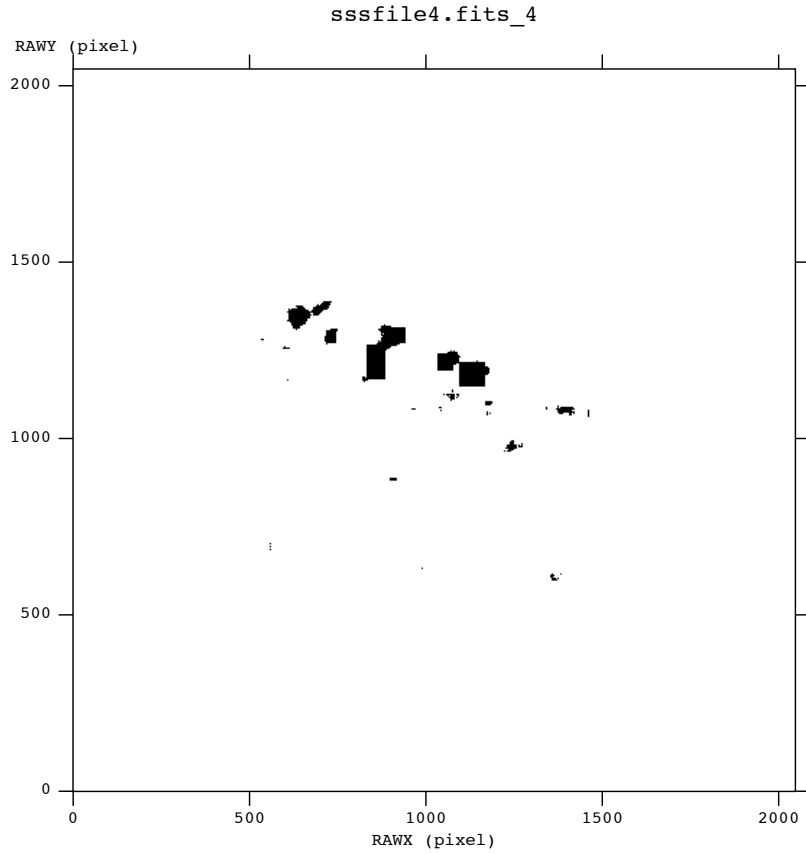

Figure 8 SSS map for UV filters. Regions of low sensitivity are in black.